Using CFD to Describe the Hydrodynamics of Internal Air-lift Reactors

Jasper M. van Baten, Jürg Ellenberger and Rajamani Krishna*

Department of Chemical Engineering, University of Amsterdam, Nieuwe Achtergracht 166, 1018 WV Amsterdam, The Netherlands

The hydrodynamics of three configurations of internal airlift reactors, two with riser diameters of 0.1 m and one with a riser diameter of 0.24 m, operating with air–water system, have been experimentally investigated for a range of superficial gas velocities. The experimental results are compared with a model using computational fluid dynamics (CFD) with Eulerian descriptions of the gas and liquid phases. Interactions between the bubbles and the liquid are taken into account by means of a momentum exchange, or drag coefficient based on a literature correlation. The turbulence in the liquid phase is described using the k-ε model. The CFD model shows good agreement with the measured data on gas holdup, liquid velocity in the downcomer and in the riser for all three configurations. The developed CFD model has the potential of being applied as a tool for scaling up.

L'hydrodynamique de trois configurations de réacteurs airlift interne, dont le diamètre de colonne montante est de 0,1 m pour deux d'entre eux et de 0,24 m pour le troisième, fonctionnant avec un système air-eau, a été étudiée de manière expérimentale pour une gamme de vitesse de gaz superficielle. Les résultats expérimentaux sont comparés à ceux d'un modèle utilisant la mécanique des fluides numérique (CFD) avec des descriptions eulériennes des phases de gaz et de liquide. Les interactions entre les bulles et le liquide sont prises en compte au moyen de l'échange de quantité de mouvement ou du coefficient de traînée basé sur une corrélation de la littérature scientifique. On décrit la turbulence dans la phase liquide à l'aide du modèle k-ε. Le modèle de CFD montre un bon accord avec les données mesurées sur la rétention de gaz, la vitesse de liquide dans le déversoir et dans la colonne montante pour les trois configurations. Le modèle de CFD mis au point pourra être appliqué en tant qu'outil pour des mises à l'échelle.

Keywords: airlift reactor, gas hold up, scale effects, computational fluid dynamics, liquid circulations.

Airlift reactors (ALR) are finding increasing applications in chemical industry, biochemical fermentation and biological wastewater treatment processes (Blenke, 1979; Chisti, 1989; Saez et al., 1998). There are two types of ALR: internal and external loop. Internal loop reactors consist of concentric tubes or split vessels, in which a part of the gas is entrained into the downcomer, whereas external loop reactors are two conduits connected at the top and the bottom, in which little or no gas recirculates into the downcomer. The part in which the sparger is located is called the riser, and the other is the downcomer. The driving force, based on the static pressure difference, or the mixture density difference, between the riser and the downcomer generates the loop liquid circulation. Compared with conventional reactors, such as stirred tank reactors or bubble columns, shear stress is relatively constant and mild throughout the reactor.

For design of an airlift reactor, it is necessary to have accurate estimates of the phase holdups and velocities in the riser and downcomer. Several literature studies have focused on the estimation of these hydrodynamic parameters (Calvo and Leton, 1991; Calvo and Leton, 1996; Camarasa et al., 2001a; Camarasa et al., 2001b; Chisti, 1989; Cockx et al., 1997; Dhaouadi et al., 1996; Heijnen et al., 1997; Marquez et al., 1999; Merchuk et al., 1996; Oey et al., 2001; Saez et al., 1998; See et al., 1999; van Benthum et al., 1999). In particular, the velocities of the liquid in the downcomer and riser are crucially dependent on the frictional losses, which in turn are determined by the geometry of the reactor and the operating conditions. Several empirical correlations have been proposed for the estimation of these hydrodynamic parameters; however, these correlations are restricted in their applicability to the geometry for which they were determined. Extrapolation to other geometries, scales and operating conditions is fraught with uncertainty.

Several recent publications have established the potential of computational fluid synamics (CFD) for describing the hydrodynamics of bubble columns (Jakobsen et al., 1997; Joshi, 2001; Krishna et al., 1999a, 2000a; Krishna and Van Baten, 2001; Krishna et al., 2000b; Krishna et al., 2001; Pan et al., 2000; Sanyal et al., 1999; Sokolichin and Eigenberger, 1999; van Baten and Krishna, 2001). The major objective of the present communication is to develop a CFD model for internal airlift reactors and to test its validity by comparison with experimental data obtained in columns of three different configurations. After checking the ability of the CFD approach to reproduce the measured data, the model is used

*Author to whom correspondence may be addressed. E-mail address: krishna@ science.uva.nl

to predict the influence of geometry and scale on the reactor hydrodynamics.

Experimental Set-up and Results

Three different configurations of an internal airlift reactor were investigated. Configuration I, consists of a polyacrylate column with an inner diameter of 0.15 m and a length of 2 m. At the bottom of the column, the gas phase is introduced through a perforated plate with 625 holes of 0.5 mm in diameter. A polyacrylate draft tube (riser) of 0.10 m inner and 0.11 m outer diameter with a height of 2.02 m is mounted into the column 0.10 m above the gas distributor. In order to avoid gas flow into the downcomer section, a gas-liquid separator is mounted at the top of the column of 1 m in height and 0.38 m in diameter.

In Configuration II, the same riser of internal diameter 0.15 m was housed in a column of 0.174 m internal diameter; the other dimensions and method of gas distribution were identical to that of Configuration I.

In Configuration III, a riser diameter of 0.24 m (inner diameter) and height of 2.02 m is housed inside a column of 0.38 m diameter; other dimensions are specified in Figure 1. The distributor is made up of 2750 holes of 0.5 mm in diameter.

The liquid velocity in the downcomer is determined by injecting,

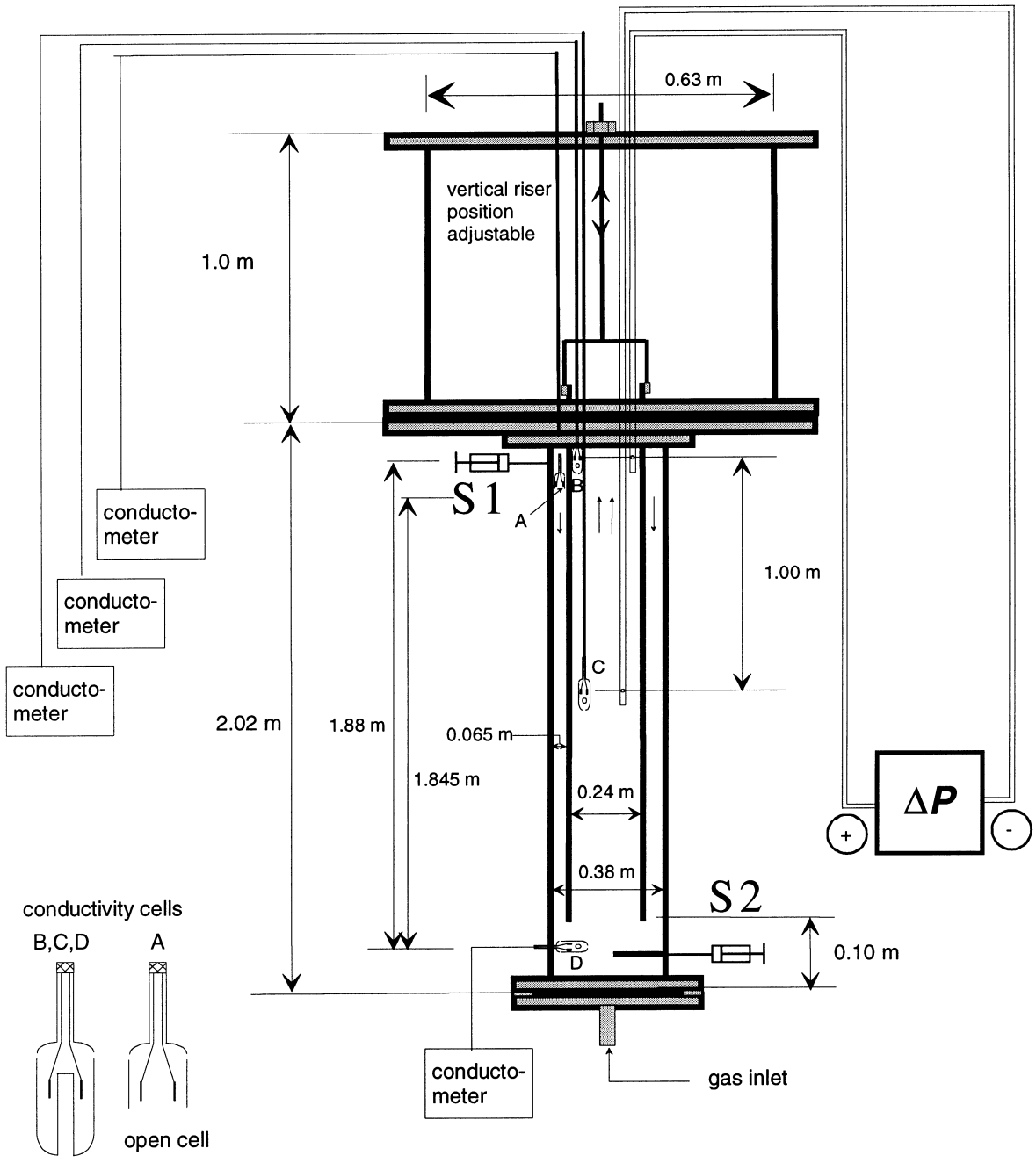

Figure 1. Experimental set up of internal airlift reactor with Configuration III.

Table 1. Properties used in the CFD simulations.

	Liquid (water)	Gas (air)
Viscosity, μ / [Pa·s]	1×10^{-3}	1.7×10^{-5}
Density, ρ/ [kg/m^3]	998	1.3
Surface tension, σ / [N/m]	0.073	

as a pulse, 1 mL of salt tracer (saturated aqueous solution of NaCl) by means of a syringe S1 at a position near the top of the downcomer. The tracer response to this salt tracer injection is measured at two positions, A and D in Figure 1, by means of conductivity cells (Metrohm) placed near the top and bottom of the downcomer, separated by a distance of 1.88 m. The conductivity cells are connected to a Consort K920 portable conductivity meter, and the transient voltage signals are recorded continuously on a PC. From the delay in the responses, Δt, the downcomer liquid velocity is determined from $1.88/\Delta t$. For determination of the liquid velocity in the riser, 1 mL of saturated aqueous solution NaCl is injected as a pulse near the bottom of the riser in the central region through a 1 mm stainless steel capillary by means of a syringe S2. The response is monitored by two conductivity probes at positions C and B, separated by a distance of 1.0 m. From the delay in the responses, Δt, the liquid velocity in the riser is determined from $1.0/\Delta t$. The gas holdup in the riser section is determined by pressure drop measurement between the same two positions, B and C, as indicated for the conductivity cells. Two closed-ended stainless steel tubes with a hole of 1.0 mm facing at a right angle to the flow direction are fixed into the riser section, the distance between the holes being 1.0 m. The pressure is transmitted through these tubes to a Validyne DP 15 pressure transducer with a range of 0 to 2200 Pa. The measuring time of the pressure signal is 120 s with a sampling frequency of 2Hz. The mean value of the pressure drop signals is used to calculate the gas holdup.

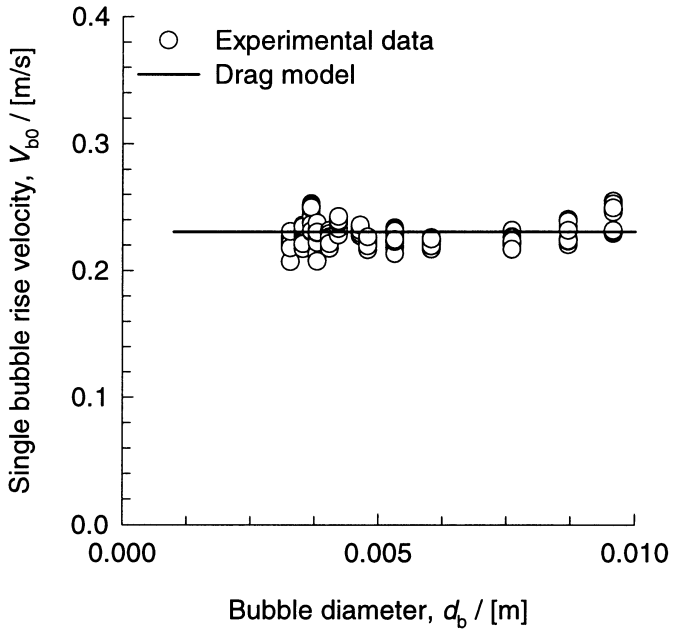

Figure 2. Experimental data on single bubble rise velocity as a function of bubble diameter (Krishna et al., 1999b), compared with predictions of the drag model adopted in this work.

Similar measurement strategies were used for Configurations I and II. All experiments in the three configurations were carried out at atmospheric pressure conditions with the air–water system. The column is filled with demineralised water to a height of 2.5 m. The hydrodynamics of the airlift system was studied for superficial gas velocities, U_G (based on the riser cross-sectional area) in the range 0.0 to 0.20 m/s. For this range of U_G values, there was no entrainment of gas in the downcomer. Also, due to the high liquid recirculations, homogenous bubbly flow was maintained in all the experiments; this could be verified visually. In the simulations, therefore, we assumed uniform bubble sizes for all the runs.

Development of CFD model

For either gas or liquid phase the volume-averaged mass and momentum conservation equations in the Eulerian framework are given by:

$$\frac{\partial(\varepsilon_k \rho_k)}{\partial t} + \nabla \cdot (\rho_k \varepsilon_k \mathbf{u}_k) = 0 \tag{1}$$

$$\frac{\partial(\rho_k \varepsilon_k \mathbf{u}_k)}{\partial t} + \nabla \cdot (\rho_k \varepsilon_k \mathbf{u}_k \mathbf{u}_k) = \mu_{k,eff}\, \varepsilon_k \left(\nabla \mathbf{u}_k + (\nabla \mathbf{u}_k)^T \right) - \varepsilon_k \nabla p + \mathbf{M}_{kl} + \rho_k \varepsilon_k \mathbf{g} \tag{2}$$

where, ρ_k, $\mathbf{u}_k$, and ε_k represent, respectively, the macroscopic density, velocity, and volume fraction of phase k; $\mu_{k,\,eff}$ is the effective viscosity of the fluid phase k, including the molecular and turbulent contributions. p is the pressure, $\mathbf{M}_{kl}$, the interphase momentum exchange between phase k and phase l and $\mathbf{g}$ is the gravitational vector.

The momentum exchange between the gas (subscript G) and liquid (subscript L) phases is given by:

$$\mathbf{M}_{L,G} = \left[\frac{3}{4} \frac{C_D}{d_b} \rho_L \right] \varepsilon_G (\mathbf{u}_G - \mathbf{u}_L) |\mathbf{u}_G - \mathbf{u}_L| \tag{3}$$

Here, the interphase drag coefficient is calculated from (Clift et al., 1978):

$$C_D = \frac{2}{3} \sqrt{E\ddot{o}} \tag{4}$$

with

$$E\ddot{o} = \frac{g(\rho_L - \rho_G) d_b^2}{\sigma} \tag{5}$$

where d_b is the equivalent diameter of the bubbles. For a single bubble rising in a quiescent liquid, the rise velocity V_{b0} can be calculated from the drag coefficient:

$$V_{b0} = \sqrt{\frac{(\rho_L - \rho_G) g}{\frac{3}{4} \frac{C_D}{d_b} \rho_L}} \tag{6}$$

The calculations of the single bubble rise velocity V_{b0} using Equations (4), (5) and (6) compare very well with the rise velocity of single air bubbles in water in a column of 0.1 m diameter (Krishna et al., 1999b); see Figure 2. We note that the rise velocity is practically independent of the bubble size in the 3 to 8 mm range. For the simulations reported here, we choose a bubble diameter d_b = 5 mm.

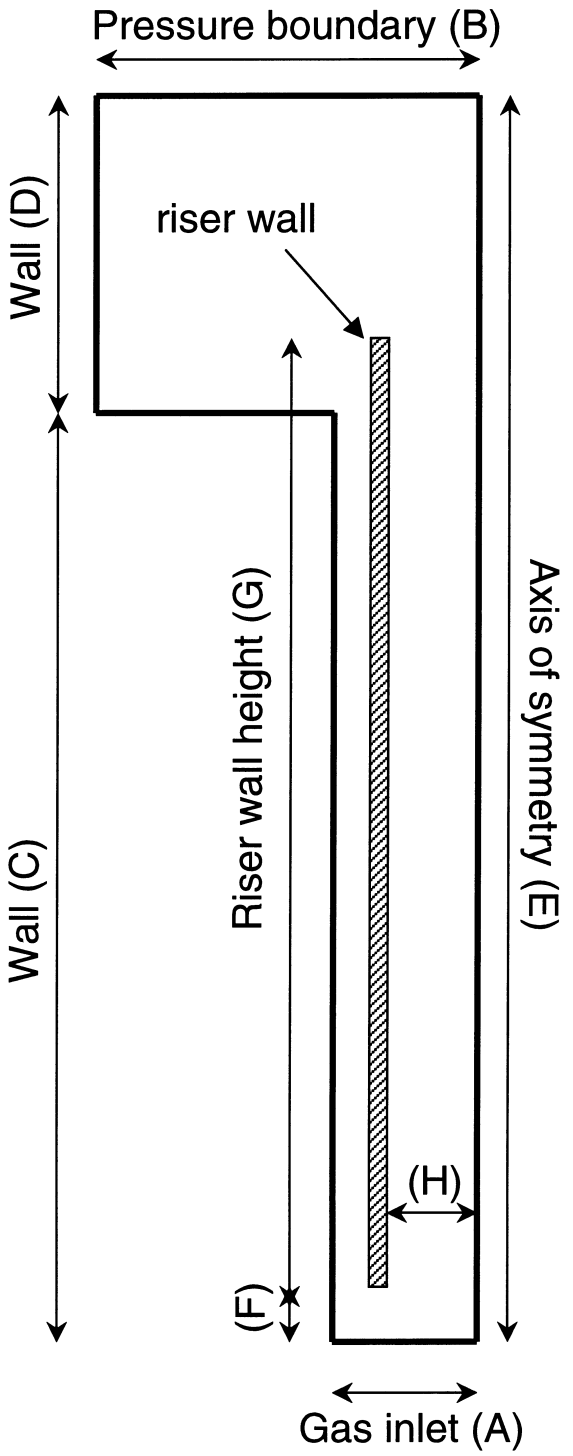

Figure 3. Computational grid details for Configurations I, II and III.

We have only included the drag force contribution to $\mathbf{M}_{L,G}$, in keeping with the works of Sanyal et al. (1999) and Sokolichin and Eigenberger (1999). The contributions of the added mass and lift forces were both ignored in the present analysis because these were verified to provide a negligible contribution.

For the continuous liquid phase, the turbulent contribution to the stress tensor is evaluated by means of k-ε model, using standard single-phase parameters C_μ = 0.09, $C_{1\varepsilon}$ = 1.44, $C_{2\varepsilon}$ = 1.92, σ_k = 1 and σ_ε = 1.3. The applicability of the k-ε model has been considered in detail by Sokolichin and Eigenberger (1999). No turbulence model is used for calculating the velocity fields inside the dispersed bubble phases.

A commercial CFD package CFX, versions 4.2 and 4.4, of AEA Technology, Harwell, UK, was used to solve the equations of continuity and momentum. This package is a finite volume solver, using body-fitted grids. The grids are non-staggered and all variables are evaluated at the cell centres. An improved version of the Rhie and Chow (1983) algorithm is used to calculate the velocity at the cell faces. The pressure-velocity coupling is obtained using the SIMPLEC algorithm (van Doormal and Raithby, 1984). For the convective terms in Equations (1) and (2), hybrid differencing was used. A fully implicit backward differencing scheme was used for the time integration.

Most of the simulations were carried out using axi-symmetric 2D grids. The computational spaces are shown in Figure 3 for Configurations I, II and III and the grid details are as specified in Table 2.

The gas was injected homogeneously over the complete bottom region (over an area equivalent to the sum of the cross-sectional areas of the riser, the downcomer and the draft tube). A pressure boundary condition was applied to the top of the column because in the experiments the top of the column is open to atmosphere. A standard no-slip boundary condition was applied at all walls. The time stepping strategy used in all simulations was 100 steps at 5×10^{-5} s, 100 steps at 1×10^{-4} s, 100 steps at 5×10^{-4} s, 100 steps at 1×10^{-3} s, 200 steps at 3×10^{-3} s, 1400 steps at 5×10^{-3} s, and 1000 steps at 1×10^{-2} s. This is more than sufficient to reach steady state, which was indicated by a situation in which all of the variables remained constant. To prevent start-up problems, the system was initialized by setting the gas holdup within the riser to 10%, and setting an initial upward velocity of 0.05 m/s in the riser, and a matching downward velocity in the downcomer.

The simulations were carried out on Silicon Graphics Power Indigo workstations with 75 MHz R8000 processors, a Silicon Graphics O2 workstation with a 150 MHz R10000 processor, and a Windows NT PC with a single Pentium Celeron processor running at 500 MHz. Each simulation was completed in about two days. Further details of the simulations are available on our Web sites: *http://ct-cr4.chem.uva.nl/airlift/* and *http://ct-cr4.chem.uva.nl/airlift38/*.

In order to test the validity of the assumption of 2D axi-symmetry, one fully three-dimensional simulation was carried out for Configuration III operating at U_G = 0.16 m/s. The 3D grid consisted of a total of 138 500 cells, with 10 cells in the azimuthal direction. The 3D simulation was carried out on a Silicon Graphics Power Challenge machine employing six R10000 processors in parallel; this simulation took 7 days to complete 10 000 time steps.

Table 2. Details of computational grids for the three-column configurations. See Figure 3 for a schematic overview of the grid geometry. The draft tube has a thickness of 0.005 m for all geometries.

Configuration	(A)	(B)	(C)	(D)	(E)	(F)	(G)	(H)	cells
I	0.075 m/15 cells	0.19 m/38 cells	2.08 m/208 cells	0.98 m/98 cells	3.06 m/306 cells	0.09 m	2.02 m	0.05 m	6844
II	0.087 m/18 cells	0.19 m/38 cells	2.08 m/208 cells	0.98 m/98 cells	3.06 m/306 cells	0.09 m	2.02 m	0.05 m	7468
III	0.19 m/38 cells	0.315 m/63 cells	2.02 m/202 cells	0.98 m/98 cells	3.00 m/300 cells	0.10 m	2.03 m	0.12 m	13850

Simulation Results and Comparison with Experiments

A typical transient approach to steady-state of the gas and liquid velocities, at the centre of the column, are shown in Figure 4 for Configuration III operating at a superficial gas velocity U_G = 0.16 m/s. Figure 4a shows that the 2D axi-symmetric simulation reaches steady state within 10 s. The steady-state values of all the hydrodynamic parameters were determined at a position 1.75 m above the distributor and reported below. The transient behaviour of the corresponding 3D simulation shows that quasi-steady state is achieved after 15 s time steps; see Figure 4b. For the 3D simulation results, time averaged values for 15 to 20 s time interval are reported below.

The steady-state radial velocity profiles, from 2D simulations, of the gas and liquid phases are shown in Figure 5 for Configurations I, II and III. For low superficial gas velocities, U_G, both gas and liquid phase can be considered to be virtually in plug flow. With increasing superficial gas velocities, both gas and liquid phases lose their plug flow character and the velocity profiles assume a parabolic shape. The parabolic velocity profile becomes more prominent with increasing riser diameter, as we move to Configuration III.

The radial distribution of gas holdup, obtained from 2D simulations are shown in Figure 6. Within the central core of the riser, the gas holdup profiles are nearly uniform over the complete range of U_G values for Configurations I and II. In Configuration II, with a larger downcomer area, there is an increase in gas holdup near the riser wall. The reason for this is that the larger sized liquid circulation cells at the riser bottom tends to move the gas towards the wall. Animations of the hydrodynamics comparing Configurations I and II, near the riser bottom on our Web site: *http://ct-cr4.chem.uva.nl/airlift/* demonstrates the reasons behind the differences in the gas holdup distribution. For Configuration III, the gas holdup shows a pronounced increase in the gas holdup at the centre of the column with increasing U_G values in this case the liquid recirculations tend to move the gas towards the center of the column as is evident in the animations on our Web site: *http://ct-cr4.chem.uva.nl/airlift38/.*

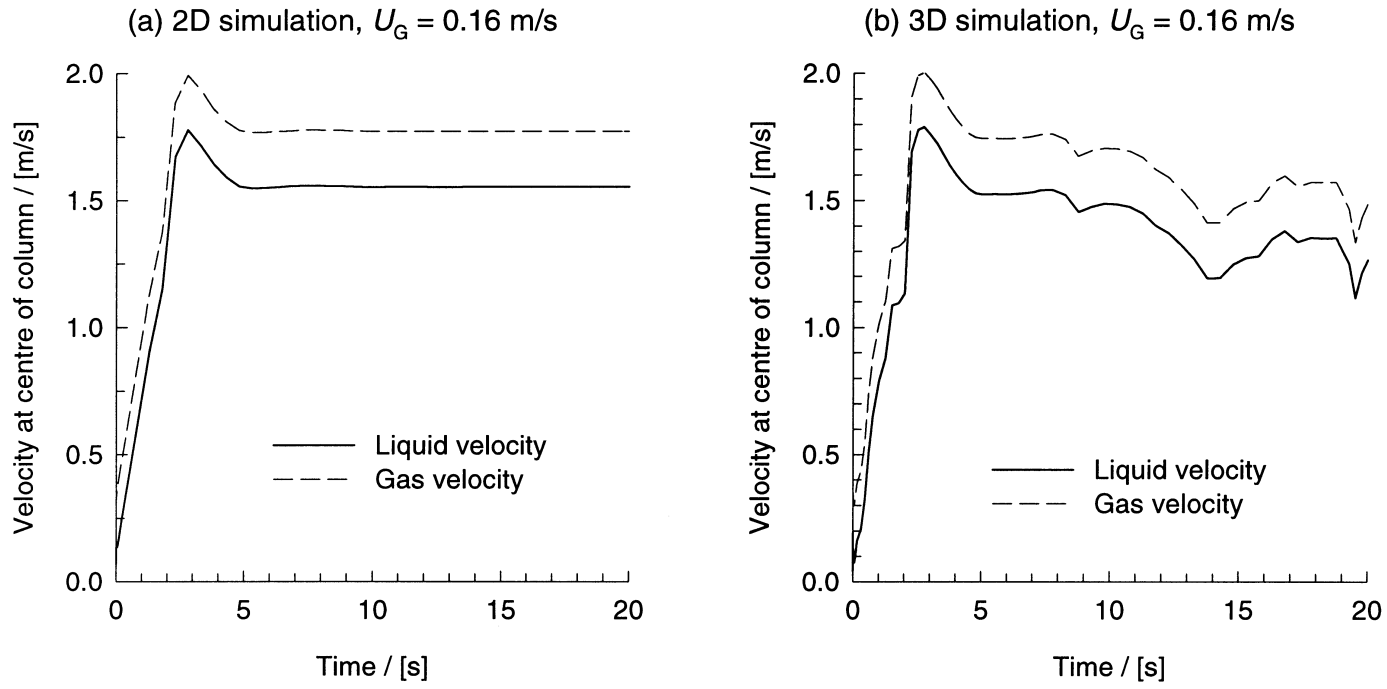

Figure 4. Transient approach to steady state of velocities and gas holdup in the riser. Simulation results for Configuration III operating at a superficial gas velocity U_G = 0.16 m/s in the riser, at a height of 1.75 m above the distributor. (a) 2D axi-symmetric simulation, and (b) 3D simulation. Animations can be viewed on the Web site: *http://ct-cr4.chem.uva.nl/airlift38/.*

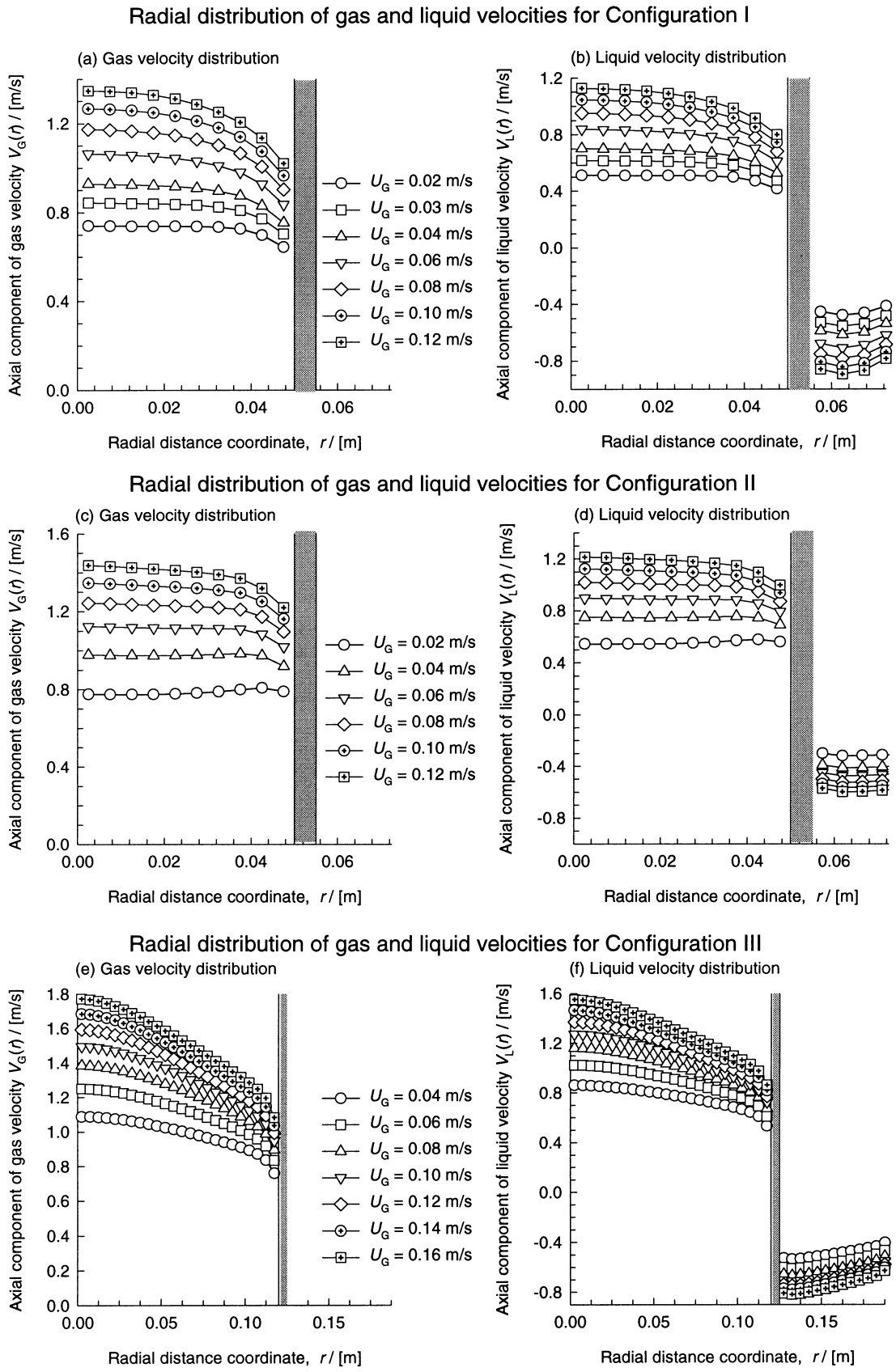

Figure 5. Radial distribution of gas velocity $V_G(r)$ and liquid velocity $V_L(r)$ for varying superficial gas velocities U_G in the riser, at a height of 1.75 m above the distributor. 2D axi-symmetric simulation results for Configurations I, II and III. Animations can be viewed on the Web site: *http://ct-cr4.chem.uva.nl/airlift/*.

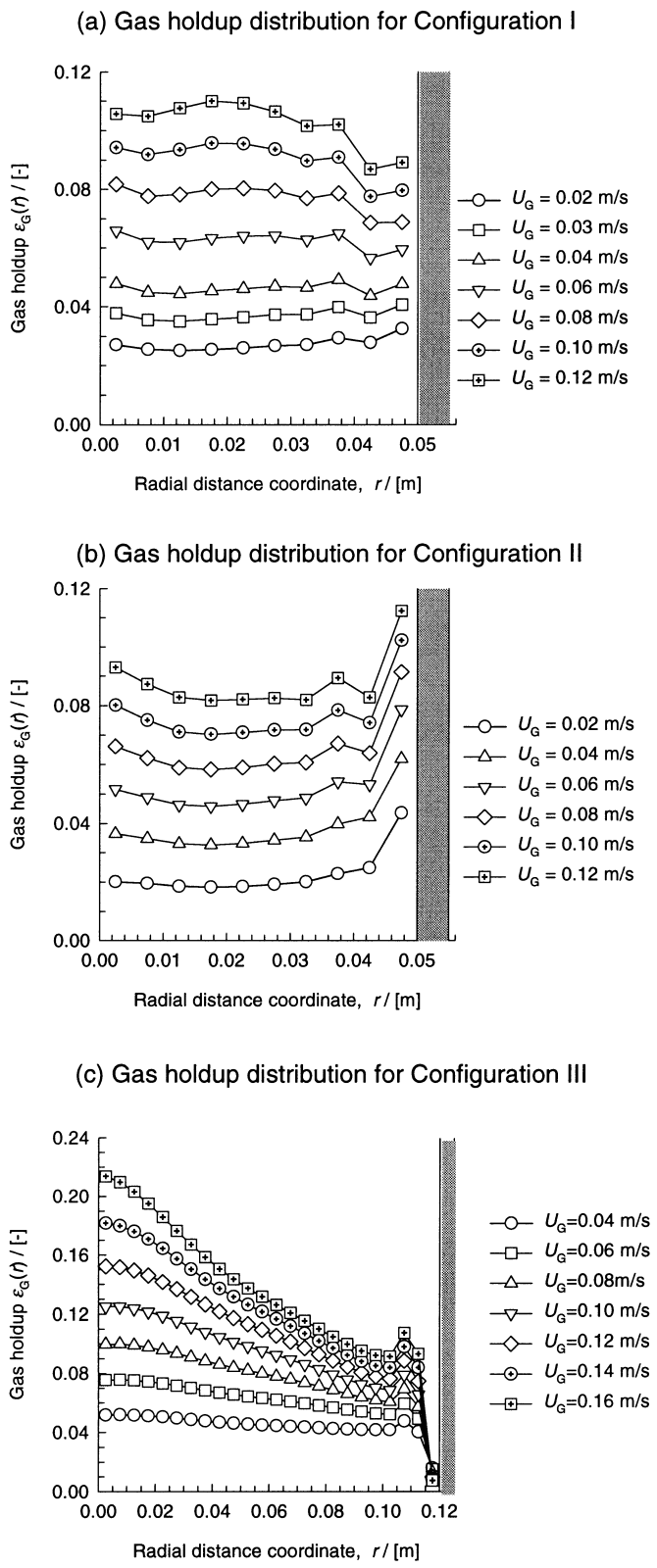

Figure 6. Radial distribution of gas holdup $\varepsilon_G(r)$ for varying superficial gas velocities U_G in the riser, at a height of 1.75 m above the distributor. 2D axi-symmetric simulation results for Configurations I, II and III. Animations can be viewed on the Web site: *http://ct-cr4.chem.uva.nl/airlift/.*

In order to check the assumption of axi-symmetry in the 2D simulations reported above, we compare the 2D and 3D simulation results for Configuration III for U_G = 0.16 m/s; see Figure 7. Forcing axi-symmetry makes the 2D simulations of the liquid velocity attain a more parabolic shape. In the 3D simulations, the gas and liquid phase slosh from side to side, as can be evidenced in the animations on our Web site: *http://ct-cr4.chem.uva.nl/airlift38/.* This side-ways sloshing makes the time-averaged velocity profiles flatter; see Figure 7a. The cross-section averaged values of the liquid velocity for the 2D

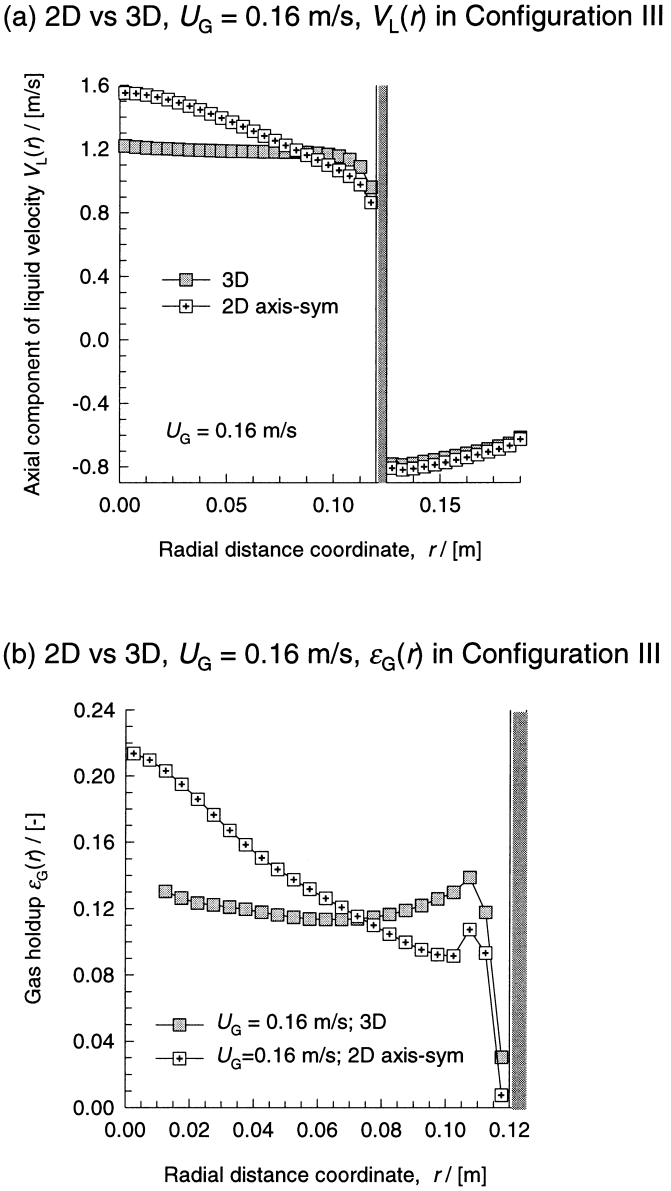

Figure 7. Comparison of 2D axi-symmetric and 3D simulation results for (a) radial distribution of liquid velocity $V_L(r)$ and (b) radial distribution of gas holdup $\varepsilon_G(r)$. Data at a height of 1.75 m above the distributor. Simulation results for Configuration III operating at a superficial gas velocity U_G = 0.16 m/s in the riser. Animations can be viewed on the Web site: *http://ct-cr4.chem.uva.nl/airlift38/.*

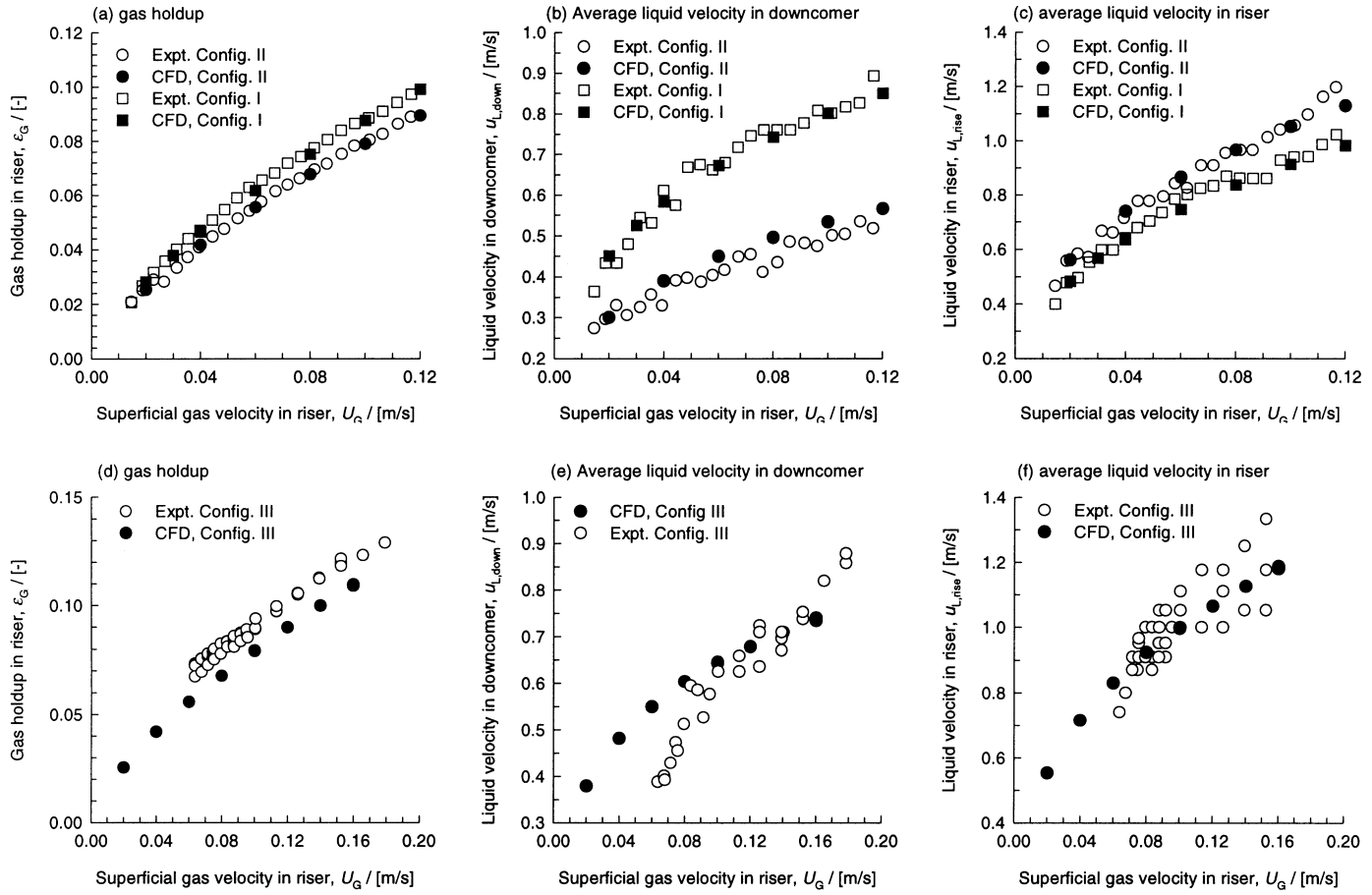

Figure 8. Comparison of experimental data and 2D axi-symmetric simulations for gas holdup in the riser, average interstitial liquid velocity in the downcomer and riser.

and 3D simulations are, respectively, 1.19 and 1.15 m/s. The gas holdup distribution for the 3D simulation is also flatter than that obtained from the axi-symmetric simulations; see Figure 7b. The cross-section averaged values of the gas holdup for the 2D and 3D simulations are, respectively, 0.109 and 0.114.

The cross-section area averaged (interstitial) liquid velocities in the riser and downcomer, and gas holdup values in the riser, obtained from the 2D axi-symmetric simulations, are compared in Figure 8 with the experimentally determined values.

Let us first compare the results for Configurations I and II, that have the same riser diameter. Configuration II has a larger downcomer area; the frictional losses are smaller and therefore a higher volume of liquid is recirculated. The higher liquid recirculations cause a smaller slip velocity between the gas and liquid phases, and consequently a smaller gas holdup. The CFD simulations are able to pick up these geometry effects very well and there is very good agreement with experiments for both Configurations I and II.

For Configuration III, both riser and downcomer areas are larger than those for Configurations I and II. Even though the right trends are predicted and the agreement between the CFD simulations and experiment is less good for Congfiguration III.

Conclusions

We have developed a CFD model to describe the hydrodynamics of an internal airlift reactor. The following major conclusions can be drawn:

- The assumption of 2D axi-symmetry leads to radial profiles of velocity that have a more parabolic character than that for fully 3D simulations. The cross-section area averaged values of gas holdup and phase velocities for 2D and 3D simulations for Configuration III are, however, close to one another; this result suggests that the assumption of axi-symmetric is valid for the geometry used in the experimental setup.
- There is good agreement between the 2D simulations and experiments; this suggests that geometry effects are properly accounted for by the CFD model.

Acknowledgements

The Netherlands Organization for Scientific Research (NWO) is gratefully acknowledged for providing financial assistance in the form of a programmasubsidie for development of novel concepts in reactive separations technology.

Nomenclature

C_D	drag coefficient
d_b	diameter of bubble, (m)
$Eö$	Eötvös number, $(g(\rho_L - \rho_G)d_b^2/\sigma)$
g	gravitational acceleration, 9.81 $(m{\cdot}s^{-2})$
$\mathbf{g}$	gravitational vector, $(m{\cdot}s^{-2})$
$\mathbf{M}$	interphase momentum exchange term, (N/m^3)
p	system pressure, (Pa)
r	radial coordinate, (m)
t	time, (s)
$\mathbf{u}$	velocity vector, (m/s)
u_L	interstitial liquid velocity, $(m{\cdot}s^{-1})$
U_G	superficial gas velocity in the riser, $(m{\cdot}s^{-1})$
$V_G(r)$	radial distribution of interstitial gas velocity, $(m{\cdot}s^{-1})$
$V_L(r)$	radial distribution of interstitial liquid velocity, $(m{\cdot}s^{-1})$
V_{b0}	single bubble rise velocity, $(m{\cdot}s^{-1})$

Greek

ε	total gas hold up
$\varepsilon_G(r)$	radial distribution of gas holdup
μ	viscosity of fluid phase, (Pa·s)
ρ	density of phase, $(kg{\cdot}m^{-3})$
σ	surface tension of liquid phase, $(N{\cdot}m^{-1})$

Subscripts

G	referring to gas
L	referring to liquid
k,l	referring to phase *k* and *l* respectively
rise	in the riser
down	in the downcomer

References

Blenke, H., "Loop Reactors", Adv. Biochem. Eng. **13**, 121–215 (1979).

Calvo, E.G. and P. Leton, "A Fluid Dynamic-Model for Bubble-Columns and Airlift Reactors", Chem. Eng. Sci. **46**, 2947–2951 (1991).

Calvo, E.G. and P. Leton, "Prediction of Gas Hold-up and Liquid Velocity in Airlift Reactors using Two-phase Flow Friction Coefficients", J. Chem. Technol. Biotechnol. **67**, 388–396 (1996).

Camarasa, E., E. Carvalho, L.A.C. Meleiro, R. Maciel, A. Domingues, G. Wild, S. Poncin, N. Midoux and J. Bouillard, "Development of a Complete Model for an Air-lift Reactor", Chem. Eng. Sci. **56**, 493–502 (2001a).

Camarasa, E., L.A.C. Meleiro, E. Carvalho, A. Domingues, R. Maciel, G. Wild, S. Poncin, N. Midoux and J. Bouillard, "A Complete Model for Oxidation Air-lift Reactors", Comput. Chem. Eng. **25**, 577–584 (2001b).

Chisti, M.Y., "Airlift Bioreactors", Elsevier Applied Science, London, UK (1989).

Clift, R., J.R. Grace and M.E. Weber, "Bubbles, Drops and Particles", Academic Press, San Diego, CA (1978).

Cockx, A., A. Line, M. Roustan, Z. DoQuang and V. Lazarova, "Numerical Simulation and Physical Modeling of the Hydrodynamics in an Air-lift Internal Loop Reactor", Chem. Eng. Sci. **52**, 3787–3793 (1997).

Dhaouadi, H., S. Poncin, J.M. Hornut, G. Wild and P. Oinas, "Hydrodynamics of an Airlift Reactor: Experiments and Modeling", Chem. Eng. Sci. **51**, 2625–2630 (1996).

Heijnen, J.J., J. Hols, R.G.J.M. van der Lans, H.L.M. van Leeuwen, A. Mulder and R. Weltevrede, "A Simple Hydrodynamic Model for the Liquid Circulation Velocity in a Full-scale Two- and Three-phase Internal Airlift Reactor Operating in the Gas Recirculation Regime", Chem. Eng. Sci. **52**, 2527–2540 (1997).

Jakobsen, H.A., B.H. Sannaes, S. Grevskott and H. F. Svendsen, "Modeling of Vertical Bubble-driven Flows", Ind. Eng. Chem. Res. **36**, 4050–4072 (1997).

Joshi, J.B., "Computational Flow Modeling and Design of Bubble Column Reactors", Chem. Eng. Sci. **56**, 5893–5933 (2001).

Krishna, R., M.I. Urseanu, J.M. van Baten and J. Ellenberger, "Influence of Scale on the Hydrodynamics of Bubble Columns Operating in the Churn-turbulent Regime: Experiments vs. Eulerian Simulations", Chem. Eng. Sci. **54**, 4903–4911 (1999a).

Krishna, R., M.I. Urseanu, J.M. van Baten and J. Ellenberger, "Liquid Phase Dispersion in Bubble Columns Operating in the Churn-Turbulent Flow Regime", Chem. Eng. J. **78**, 43–51 (2000a).

Krishna, R., M.I. Urseanu, J.M. van Baten and J. Ellenberger, "Wall Effects on the Rise of Single Gas Bubbles in Liquids", Int. Commun. Heat Mass Transf. **26**, 781–790 (1999b).

Krishna, R. and J.M. Van Baten, "Scaling up Bubble Column Reactors with the Aid of CFD", Chem. Eng. Res. Des. **79**, 283–309 (2001).

Krishna, R., J.M. van Baten and M.I. Urseanu, "Three-phase Eulerian Simulations of Bubble Column Reactors Operating in the Churn-Turbulent Regime: a Scale up Strategy", Chem. Eng. Sci. **55**, 3275–3286 (2000b).

Krishna, R., J.M. van Baten, M.I. Urseanu and J. Ellenberger, "Design and Scale up of a Bubble Column Slurry Reactor for Fischer-Tropsch Synthesis", Chem. Eng. Sci. **56**, 537–545 (2001).

Marquez, M.A., R.J. Amend, R.G. Carbonell, A.E. Saez and G.W. Roberts, "Hydrodynamics of Gas-lift Reactors with a Fast, Liquid-phase Reaction", Chem. Eng. Sci. **54**, 2263–2271 (1999).

Merchuk, J.C., N. Ladwa, A. Cameron, M. Bulmer, I. Berzin and A.M. Pickett, "Liquid Flow and Mixing in Concentric Tube Air-lift Reactors", J. Chem. Technol. Biotechnol. **66**, 174–182 (1996).

Oey, R.S., R.F. Mudde, L.M. Portela and H.E.A. van den Akker, "Simulation of a Slurry Airlift using a Two-fluid Model", Chem. Eng. Sci. **56**, 673–681 (2001).

Pan, Y., M.P. Dudukovic and M. Chang, "Numerical Investigation of Gas-driven Flow in 2-D Bubble Columns", AIChE J. **46**, 434–449 (2000).

Rhie, C.M. and W.L. Chow, "Numerical Study of the Turbulent Flow Past an Airfoil with Trailing Edge Separation", AIAA J. **21**, 1525–1532 (1983).

Saez, A.E., M.A. Marquez, G.W. Roberts and R. G. Carbonell, "Hydrodynamic Model for Gas-lift Reactors", AIChE J. **44**, 1413–1423 (1998).

Sanyal, J., S. Vasquez, S. Roy and M. P. Dudukovic, "Numerical Simulation of Gas-liquid Dynamics in Cylindrical Bubble Column Reactors", Chem. Eng. Sci. **54**, 5071–5083 (1999).

See, K.H., G.W. Roberts and A.E. Saez, "Effect of Drag and Frictional Losses on the Hydrodynamics of Gas-lift Reactors", A.I.Ch.E.J. **45**, 2467–2471 (1999).

Sokolichin, A. and G. Eigenberger, "Applicability of the Standard k-epsilon Turbulence Model to the Dynamic Simulation of Bubble Columns: Part I. Detailed numerical simulations", Chem. Eng. Sci. **54**, 2273–2284 (1999).

van Baten, J.M. and R. Krishna, "Eulerian Simulations for Determination of the Axial Dispersion of Liquid and Gas Phases in Bubble Columns Operating in the Churn-turbulent Regime", Chem. Eng. Sci. **56**, 503–512 (2001).

van Benthum, W.A.J., R. van der Lans, M.C.M. van Loosdrecht and J. J. Heijnen, "Bubble Recirculation Regimes in an Internal-loop Airlift Reactor", Chem. Eng. Sci. **54**, 3995–4006 (1999).

van Doormal, J. and G.D. Raithby, "Enhancement of the SIMPLE Method for Predicting Incompressible Flows", Numer. Heat Transfer **7**, 147–163 (1984).

Manuscript received September 19, 2002; revised manuscript received April 8, 2003; accepted for publication May 22, 2003.